Intrinsic versus shape anisotropy in micro-structured magnetostrictive thin films for magnetic surface acoustic wave sensors

Harshad Mishra[1], Michel Hehn[1], Daniel Lacour[1], Omar Elmazria[1], Nicolas Tiercelin[2], Hamid Mjahed[1], Karine Dumesnil[1], Sebastien Petit Watelot[1], Vincent Polewczyk[1], Abdelkrim Talbi[2], Olivier Bou Matar[2], Sami Hage-Ali[1]

[1]Institut Jean Lamour, Université de Lorraine, UMR CNRS 7198, F-54000 Nancy, France
[2]Univ. Lille, CNRS, Centrale Lille, ISEN, Univ. Valenciennes, UMR 8520 – IEMN, LIA LICS/LEMAC, F-59000 Lille, France

E-mail : harshad.vr1@gmail.com

Received xxxxxx
Accepted for publication xxxxxx
Published xxxxxx

Abstract

This work aims at studying the interaction between surface acoustic waves (SAW) and micro-structured magnetostrictive layers under a magnetic field with a perspective to develop magnetic field sensors. The impact of the competition between the strong intrinsic magnetic anisotropy of the magnetic material and the shape anisotropy of the interdigitated transducer (IDT) fingers introduced by the micro-structuration is investigated. Therefore, the macroscopic and microscopic magnetic properties of the IDT and their influence on the magneto-acoustic response are studied. A SAW resonator with the IDTs made of the magnetostrictive thin film was elaborated and the magnetic surface acoustic wave (MSAW) response under a magnetic field was performed and discussed. Depending on the energy balance, the anisotropy gets modified and a correlation with the MSAW sensitivity to an externally applied magnetic field is made.

Keywords: saw sensors, magnetic, shape-effects, micromagnetics, micro-structured thin films

1. Introduction

Magnetic sensors that are available in the market today are not only expensive, but also require external power supplies for operation. Some of these devices are also quite bulky and limited in terms of space and usability. Thus, Surface Acoustic Wave (SAW) sensors appear as reliable low profile, passive devices. The ease of coupling with antennas allows SAW devices to be interrogated wirelessly [1,2] while a multilayered structure allows packageless operation [3]. Temperature [4,5] strain [6], gas [7,8,9], humidity [10,11], pressure sensors [12,13,14] and even bio-sensing [15,16] have been the subject of many developments using SAW sensors showing that multisensory platforms can be developed. The implementation of magnetic materials in SAW sensors extended the measurement potential to magnetic fields through field-dependent strain induced by magnetization rotation in magnetostrictive materials [17,18,19]. The effect, referred to as the magnetoelectric delta-E effect, requires an accurate control of the easy axis of magnetization, both in direction and intensity. Studies conducted by Elhosni *et al.* [20] and Zhou *et al.* [21,22] have shown the possibility to

realize magnetic SAW (MSAW) sensors with a delay line configuration using a layered structure through a control of the easy axis of magnetization of the magnetic layer with respect to the acoustic wave propagation direction . Finite element based studies done by Elhosni *et al.* [23] also proved that high sensitivity may be achieved through proper selection of materials, especially the magnetic material, by decreasing the anisotropy field. SAW resonators with Ni interdigitated transducers (IDTs) were investigated by Kadota *et al.* [24]. Kadota *et al.* [24], Yamaguchi *et al.* [25] and Smole *et al.* [26] have also attempted to describe the physical phenomenon behind the sensor behaviour without any magnetic characterisation of the IDT. In our last report [27] we showed that the shape anisotropy induced in the magnetic IDT can reorient the easy axis of magnetization along the IDT length when the magnetic material is soft, limiting delta-E effects to geometries with applied fields along the acoustic wave propagation. By the use of 25×[$TbCo_2$/FeCo] exchange coupled multilayers, a material known to have a high magnetic anisotropy induced by applying a magnetic field during deposition [21,22,28], we show that magnetic sensitivity can be kept with applied field along the IDT. The comparison between the macroscopic and microscopic magnetic properties of the IDT shows that a complex domain structure develops due to the competition between intrinsic and shape anisotropies but leading to MSAW response characteristic of a hard axis response. So, we aim to explain the relation between the magnetic anisotropy of the sensitive IDTs and the MSAW response, and explore the implications regarding magnetic SAW sensors engineering.

2. Experiments

2.1 Fabrication

200nm of [$TbCo_2$(4nm)/FeCo(4nm)]×25 was deposited on a 128° Y-cut $LiNbO_3$ (LN-128) substrate by RF sputtering using a Laybold Z550 frame. The layers are obtained by sputtering composite targets: one composed of Co with pellets of Tb for the $TbCo_2$ layer and the other composed of an Fe target with Co pellets for the FeCo layer. The sputtering was carried out under a bias magnetic field of approximately 100 Oe to induce a preferential magnetic anisotropy direction (Easy Axis or EA) parallel to the (X+90°) direction of the crystalline substrate (figure 1(a)).

From the full film, synchronous single port SAW resonators were patterned using photolithography and dry Ar Ion Beam Etching (IBE) with a device wavelength (λ) of 6.5µm (figure 1(b)). The SAW samples are labelled D (for Device). In order to measure the magnetic response of the IDTs, samples composed of only IDT fingers were also fabricated and are labelled V (for VSM). The devices were also fabricated with two different orientations of the wave propagation Q: (i) Q parallel and so IDT perpendicular to the EA of the full film (MSAW sample $D_{IDT\perp EA}$ and sample for magnetic characterization $V_{IDT\perp EA}$) and (ii) Q perpendicular and so IDT parallel to the EA of the full film (MSAW sample $D_{IDT//EA}$ and sample for magnetic characterization $V_{IDT//EA}$). Finally, since shape effects are linked to the width of the IDT fingers, 2 different metallization ratios (relative widths of the IDTs with respect to the device wavelength) have been tested (40% and 60%) for the magnetometry. The two metallization ratios allow us to monitor two different IDT widths.

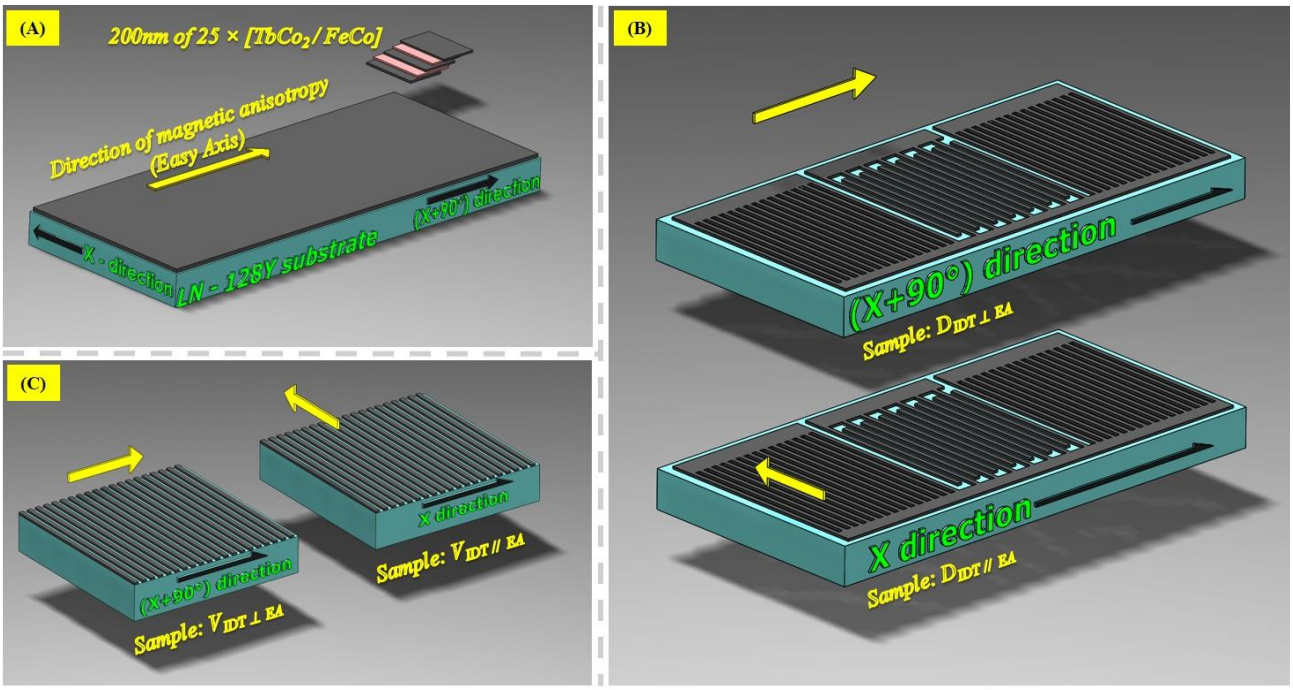

Figure 1: (a) Schematic of the sample configuration (full film) before lithography with the relevant directions. The inset shows the multi-layered structure of the film. (b) MSAW devices (100pairs of IDT and 200 reflectors on each side) and (c) the corresponding sample for magnetometry. The yellow arrow corresponds to the easy magnetization axis of the full film.

2.2 Magnetometry

As a first step, vibrating sample magnetometer (VSM) measurements were carried out to determine the magnetic response of the full film. It presents a well-defined anisotropy along the (X+90°) direction and presents a hysteresis free reversal along X, the hard axis, with an anisotropy field close to 1690 Oe (green curves figure 2(a) and (b)) and a square hysteretic reversal when the field is applied along (X+90°) (green curves figure 2(c) and (d)). A saturation magnetization value of 497×10^3 A/m was thus extracted for the full film.

In the second step, the full film was shaped into IDTs with the finger length along X+90°, i.e. parallel to the easy axis of the full film (sample $V_{IDT//EA}$) and the VSM test repeated. As expected from a previous study [27] and micromagnetism theory, the easy axis of magnetization remains along X+90°.

Sample $V_{IDT\perp EA}$ presents a hard axis response along X (black curves figure 2(a) and (b)) and a square hysteretic

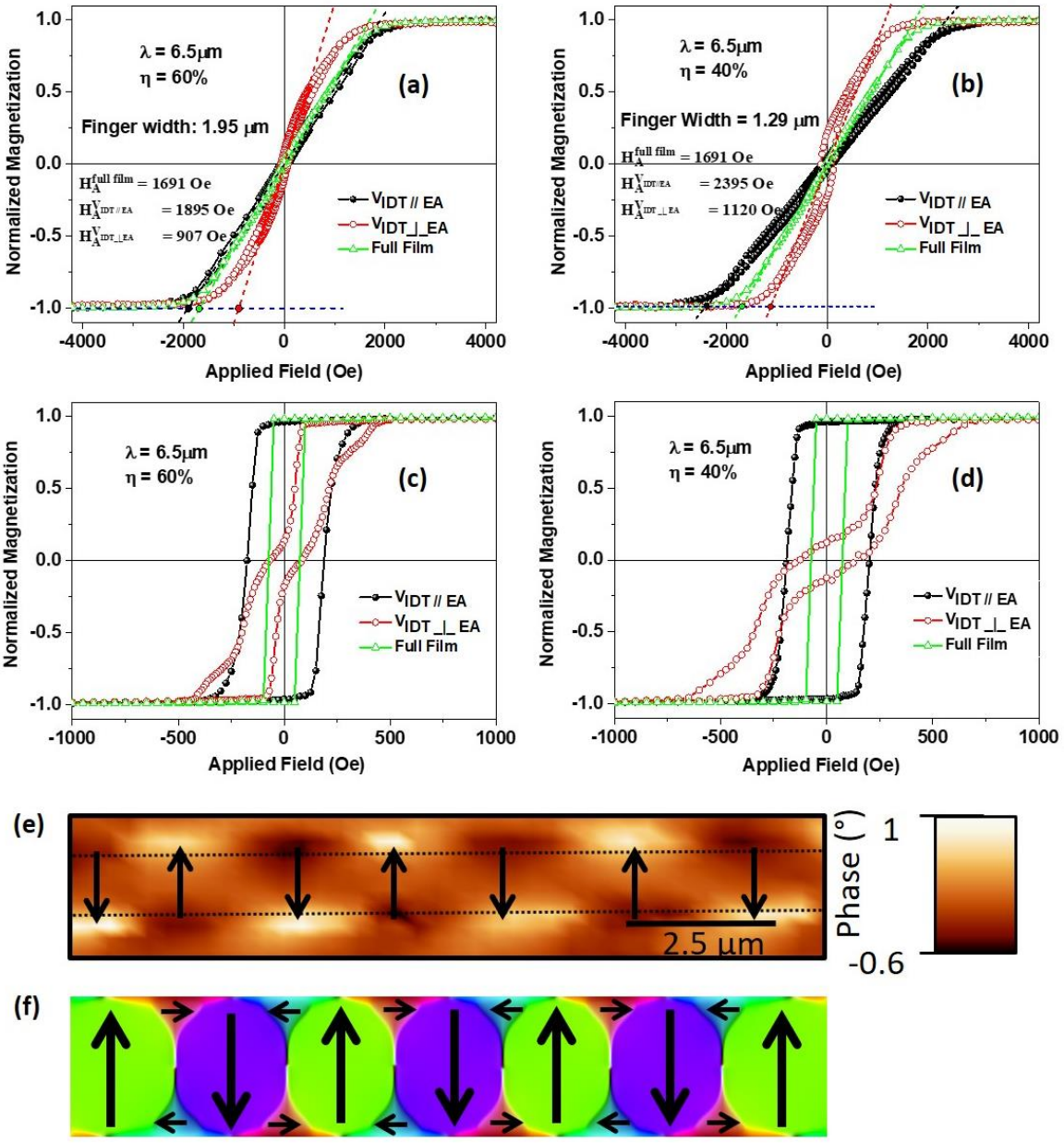

Figure 2: Normalized magnetization curves measured for the full film (green), for IDTs oriented parallel to the (X+90°) easy axis of the full film (black), and for IDTs oriented along X, perpendicular to the easy axis of the full film (red). Figures (a) and (c) report the measurements of IDTs with a metallization ratio of 60% ((b) and (d) those for 40%). Top figures (a) and (b) report measurements with the applied field along X and the bottom figures (c) and (d) report measurements with the applied field along X+90°.

(e) MFM measurements on IDTs fabricated perpendicular to the anisotropy direction (Sample- $V_{IDT\perp EA}$). The dotted lines show the boundary of the IDT finger. (f) Domain structure calculated for a 12.5μm long and 200nm thick finger with: saturation magnetization of 500×10^3 A/m and finger width of 2μm.

reversal when the field is applied along (X+90°) (black curves figure 2(c) and (d)). The intrinsic anisotropy of the full film should thus be reinforced by the shape induced anisotropy. A rough estimation of the induced shape anisotropy field is 704 Oe for the 1.29 µm wide fingers (40% of metallization) and 204 Oe for the 1.95 µm wide fingers (60% of metallization). We can clearly see that the effective anisotropy field is higher but the reinforcement due to shape is not as high as expected. A measure of the saturation magnetization of the fingers, by taking the volume of the fingers into account (as measured through Atomic Force Microscopy) led to a value of 498×10^3 A/m, close to the value obtained for the full film (505×10^3 A/m).

Subsequently, the full film was shaped into IDTs with the finger length oriented along X, i.e. perpendicular to the easy axis of the full film. This sample is referred to as $V_{IDT\perp EA}$ and its magnetic response is reported by red curves in figure 2. Even if a shape anisotropy that competes with the intrinsic anisotropy of the thin film is introduced here, the $V_{IDT\perp EA}$ sample still presents a hard axis response along X (red curves figure 2(a) and (b)). The magnetic response along X+90° shows an abnormal wavy response (red curves in figure 2(c) and (d)) with a magnetic remanence close to zero. Such kind of response is symptomatic of the creation of a domain structure at zero applied field. Therefore, magnetic force microscopy (MFM) has been performed and a zoom on one IDT is reported in figure 2(e). A domain structure can be observed with alternating black and white contrast on the IDT finger border. In order to undoubtedly interpret the MFM contrast, micromagnetic calculations have been performed using the Mumax3 code [29]. The average parameters of the [$TbCo_2$(4nm)/FeCo(4nm)]×25 multilayer have been used: saturation magnetization value of 500×10^3 A/m, exchange stiffness of 9×10^{-12} J/m and second order anisotropy of 48.25×10^3 J/m^3 orientated in plane and perpendicular to the finger length. The cell size has been fixed to 5nm. The configurations have been relaxed starting from the saturated state along the finger length. The micromagnetic configuration is reported in figure 2(f). Undoubtedly, the magnetization lies along the easy axis of the full film i.e. perpendicular to finger length. A domain configuration is stabilized in order to reduce the demagnetization energy as previously reported [30]. The surface charges are reduced by the creation of the red and blue flux closure domains. Those domains are at the origin of the hysteresis of the magnetic response observed when the field is applied along X (red curves figure 2(a) and (b)). When finger width decreases, the magnetization remains along the easy axis of magnetization of the full film but domain size decreases. As a result, a domain structure is stabilized in fingers with different metallization ratios tested in our study (40% and 60%).

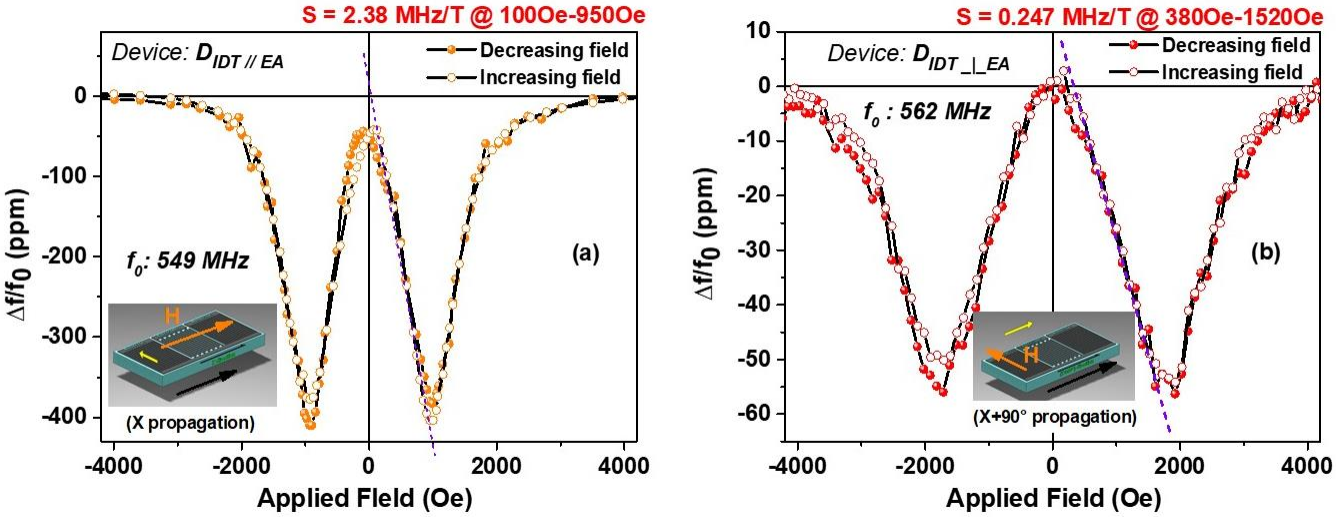

Figure 3: (A) Relative variation of the resonance frequency for device $D_{IDT//EA}$ (λ = 6.5um, η = 60%; EA // IDT) when a magnetic field is applied perpendicular to the easy axis. (B) Relative variation of the resonance frequency for device $D_{IDT\perp EA}$ (λ = 6.5um, η = 60%, EA _|_ IDT) when a magnetic field is applied perpendicular to the easy axis.

2.3 MSAW Measurement

The resonant frequencies of the fabricated devices were determined from their S_{11} scattering parameters measured using a network analyser (Agilent PNA 5230A, Santa Clara) and RF probe station (PM5 Suss Micro-Tech). The MSAW measurements were made using a LakeShore cryogenic probe station (EMPX-HF) connected to a VNA (Rohde and Schwartz ZVA67) by a K-cable and GGB Picoprobes (40GHz). Since the magnetostriction-induced variation of the

resonator operating frequency is expected to be the strongest when the moments rotate towards the applied magnetic field, only the experiments with the field applied along the magnetic hard axis (X) are reported in the following. The variations of the resonance frequencies (relative shift) when a magnetic field is applied along X with maximum field value of 4 kOe are shown in figure 3. Device $D_{IDT//EA}$, which has Rayleigh waves propagating along the X direction exhibits a frequency variation typically observed when the field is applied along a hard magnetization axis and shows a sensitivity of 2.38 MHz/T in the [100 Oe - 950 Oe] range. Device $D_{IDT\perp EA}$ on the other hand shows a sensitivity of 0.247 MHz/T for the Rayleigh wave in the [380 Oe-1520 Oe] field range. There is an additional Shear-Horizontal component in this configuration (Device $D_{IDT\perp EA}$). However, it is neglected from this study to focus exclusively on the Rayleigh wave.

As far as the Rayleigh waves are concerned, the MSAW response depends on the relative orientations for wave propagation and magnetic anisotropy directions (figure 3 (a) & (b)). Since it has a direct dependency on the magnetization, it may also be noted that adjusting the width of the IDT will also lead to a control of the MSAW response. For this wave, the minimum frequency is expected at the point of maximum magneto-mechanical coupling (K^2) that occurs when the angle between the applied field and the moment is 45° [31]. Assuming a magnetization rotation in a Stoner-Wohlfarth type when the field is applied along the hard axis, this happens when magnetization reaches 70% of the saturation magnetization. By the use of magnetic responses for the IDT given in figure 2(a) (red & black curves), those fields are 870 Oe for $V_{IDT\perp EA}$ and 1340 Oe for $V_{IDT//EA}$. Those values are in agreement with the measurements performed on the SAW devices (869 Oe for $D_{IDT\perp EA}$ and 1814 Oe for $D_{IDT//EA}$). This difference in saturation fields partially explains the difference in magnetic sensitivity between $D_{IDT\perp EA}$ and $D_{IDT//EA}$. Another difference is the SAW propagation direction, parallel to X+90° in $D_{IDT\perp EA}$ and parallel to X in $D_{IDT//EA}$.

3. Conclusion

In conclusion, we have shown that the shape effects in magnetism do indeed play a crucial role in influencing the acoustic behaviour of a resonator type SAW sensor. This effect may be used in combination with appropriately selected materials, to engineer a sensor with a given sensitivity in a desired magnetic field range. This study also paves the way to future investigation of the intricate relations between magnetic anisotropy direction, SAW propagation direction and the nature of the substrate.

Acknowledgements

We would like to acknowledge the support from the French PIA project “Lorraine Université d’Excellence” (ANR-15-IDEX-04-LUE) and by the Région Lorraine, ANR JCJC SAWGOOD (ANR-18-CE42-0004-01) the European funds FEDER. Experiments were carried out on IJL Project TUBE-Davm equipment funded by FEDER (EU), Region Grand Est, Metropole Grand Nancy. We also extend our sincere gratitude to the staff from the Competence Centre MINALOR for helpful discussions in fabrication. Magnetic multilayers were grown in the cleanroom facilities at IEMN, supported by the RENATECH Network.

References

[1] Reindl L., Scholl G., Ostertag T., Ruppel C.C.W., Bulst W.-E. and Seifert F., 1996 Proc. IEEE Ultrasonics Symp. 363
[2] Malocha D.C., Gallagher M., Fisher B., Humphries J., Gallagher D. and Kozlovski N., 2013 Sensors 13 5897
[3] Elmazria O., Zhgoon S., Le Brizoual L., Sarry F., Tsimbal D. and Djouadi M.A. 2009 Appl. Phys. Lett. 95 233503
[4] Aubert T., Elmazria O., Assouar B., Bouvot L. and Oudich M. 2010 Appl. Phys. Lett. 96 203503
[5] Aubert T., Bardong J., Legrani O., Elmazria O., Assouar B., Bruckner G. and Talbi A. 2013 J. Appl. Phys. 114 014505
[6] Eun K., Lee K. J., Lee K. K., Yang S. S. and Choa Sung-Hoon 2016 Int. J. Precision Engg. & Manufacturing 17 699
[7] Devkota J., Ohodnicki P. R. and Greve D. W. 2017 Sensors 17 801
[8] Liu J. and Lu Y. 2014 Sensors 14 6844
[9] Jakubik W. P. 2011 Thin Solid Films 520 986
[10] Guo Y. J., Zhang J., Zhao C., Hu P.A., Zu X. T. and Fu Y. Q. 2014 Optik 125 5800
[11] Xuan W., He M., Meng N., He X., Wang W., Chen J., Shi T., Hasan T., Xu Z., Xu Y. and Luo J.K. 2014 Sci. Rep. 4 7206
[12] Rodriguez-Madrid J. G., Iriarte G. F., Williams O.A. and Calle F. 2013 Sens. Act. A: Phys 189 364
[13] Nicolay P., Elmazria O., Sarry F., Bouvot L., Marche N. and Kambara H. 2008 Appl. Phys. Lett. 92 141909
[14] Houri C.G., Talbi A., Viard R., Moutaouekkil M., Elmazria O., Gallas Q., Garnier E., Merlen A. and Pernod P. 2017 Appl. Phys. Lett. 111 113502
[15] Gray E. R., Turbe V., Lawson V.E., Page R.H., Cook Z.C., Ferns R.B., Nastouli E., Pillay D., Yatsuda H., Athey D. and McKendry R.A. 2018 npj Dig. Med. 1 35
[16] Brooks J., Bufacchi R., Kondoh J., Duffy D.M. and McKendry R.A. 2016 Sens. Act. B: Chem 234 412
[17] Tong J., Jia Y., Wang W., Wang Y., Wang S., Liu X. and Lei Y. 2017 Appl. Sci. 7 755
[18] Li W., Dhagat P. and Jander A. 2012 IEEE Trans. Magn. 48 4100
[19] Liu X., Tong B., Ou-Yang J., Yang X., Chen S., Zhang Y. and Zhu B. 2018 Appl. Phys. Lett. 113 082402
[20] Elhosni M., Elmazria O., Petit-Watelot S., Bouvot L., Zhgoon S., Talbi A., Hehn M., Aissa K. A., Hage-Ali S., Lacour D., Sarry F. and Boumatar O. 2016 Sensors and Actuators A 240 41
[21] Zhou H., PhD Thesis 2014 Ecole Centrale de Lille
[22] Zhou H., Talbi A., Tiercelin N. and Bou Matar O. 2014 Appl. Phys. Lett. 104 114101

[23] Elhosni M., Petit-Watelot S., Hehn M., Hage-Ali S., Aissa K.A., Lacour D., Talbi A. and Elmazria O. 2014 Procedia Eng. 87 408
[24] Kadota M., Ito S., Ito Y., Hada T. and Okaguchi K. 2011 Jpn. J. Appl. Phys. 50 07HD07
[25] Yamaguchi M., Hashimoto K.Y., Kogo H. and Naoe M. 1980 IEEE Trans. Mag. 16 5
[26] Smole P., Ruile W., Korden C., Ludwig A., Quandt E., Krassnitzer S. and Pongratz P. 2003 Proc of IEEE Int. Freq. Ctrl. Sym. & PDA Exhibition
[27] Polewczyk V., Dumesnil K., Lacour D., Moutaouekkil M., Mjahed H., Tiercelin N., Petit-Watelot S., Mishra H., Dusch Y., Hage-Ali S., Elmazria O., Montaigne F., Talbi A., Bou Matar O. and Hehn M. 2017 Phys. Rev. Applied 8 024001
[28] Youssef J. B., Tiercelin N., Petit F., Le Gall H., Preobrazhensky V.and Pernod P. 2002 IEEE Trans. Mag. 38 5 2817
[29] Vansteenkiste A., Leliaert J., Dvornik M., Helsen M., Garcia-Sanchez F. and Waeyenberge B.V. 2014 AIP Advances 4 107133
[30] Prejbeanu L., PhD thesis 2001 Université de Louis Pasteur de Strasbourg
[31] Dreher L., Weiler M., Pernpeintner M., Huebl H., Gross R., Brandt M.S. and Goennenwein T. 2012 Phys. Rev. B 86 134415
[32] Polewczyk V., PhD thesis 2018 Université de Lorraine